

## Determination of local thermal conductivity of soldered joints of InGaP/Ga(In)As/Ge heterostructure with heat-dissipating AlN ceramics based on Sn42Bi58 alloy by laser photodeflection microscopy

© A.L. Glazov, V.S. Kalinovskii, A.A. Kapralov, E.V. Kontrosh, K.L. Muratkov, K.K. Prudchenko

Ioffe Institute, St. Petersburg, Russia  
E-mail: glazov.holo@mail.ioffe.ru

Received September 16, 2024

Revised October 25, 2024

Accepted October 26, 2024

The method of laser scanning photodeflection microscopy was used to study heat flows through soldered joints in the kilohertz modulation range. Local thermal conductivities inside the solders made using flux and fluxless solders based on the eutectic alloy Sn42Bi58 were estimated. It was shown that the thermal conductivity of the solder differs from the tabular thermal conductivity of the alloy and depends on the type of solder and soldering technology. Increasing the pressure on the elements being joined during soldering allows reducing the thermal resistance of the solder.

**Keywords:** lead-free solders, thermal resistance, temperature waves, scanning microscopy.

DOI: 10.61011/TPL.2025.02.60640.20123

The tightening of environmental regulations in industry, including electronics, has led to a decreased use of lead-containing solders, despite their popularity and good physical and mechanical properties. Therefore, lead-free alloys with suitable properties are being widely researched. Most of the proposed alloys have a melting point higher than that of standard lead-tin solder, which is a major problem in the production of a large range of electronic devices [1]. Alloys based on bismuth and indium [2,3] have a much lower melting point. There is much interest in using such alloys in microelectronic devices as thermal interface materials for heat transfer, for example, from multijunction solar cells and  $p-i-n$ -photodetectors to the heat sink. Sn–Bi–In based alloys have been actively studied in terms of microstructure and mechanical properties, but their thermal conductive properties are poorly understood. Meanwhile, the efficiency of the thermal management system is largely limited by the thermal conductivity of the junction. In general, obtaining information on the actual thermal characteristics of the solder contact is of great interest for the development and performance evaluation of electronic devices [4,5]. It should be noted that to characterize the thermal quality of the contact requires not only its average thermophysical parameters, but also their local values. Local deterioration of heat removal from the contact can lead to its overheating, the occurrence of thermal stresses and eventually to the destruction of the contact. A common cause of this is the formation of voids within the solder in case of current [6] flows.

Bismuth — is a nontoxic and widespread metal. Alloys based on bismuth and tin proved to be quite promising due to a combination of good thermal and physical-mechanical properties and economic efficiency [7]. A unique property of this alloy is low viscosity, comparable

to the water viscosity. To improve the microstructure and increase its homogeneity, various alloying additives Sn–Bi are introduced into the [8,9] alloy. Due to its good wettability with different surfaces, developers would like to reinforce this alloy with nanotubes [10].

In [11], the diffusivity and thermal conductivity coefficients of seven Sn–Bi alloys of different quantitative compositions were measured. To do this, samples of 2 mm thickness made of high-purity tin and bismuth in different proportions were used. At the same time, the thickness of the junction in modern devices varies within a few tens of micrometers. In addition, its microstructure and thermal resistance in general are influenced by the interaction of solder with the metallized layers of the components to be joined. The study of thermal conductivity of such contacts in the finished device by traditional methods, such as the flash [12] method, is virtually impossible. Therefore, in this study, laser scanning microscopy with photodeflection (PD) registration of temperature waves [13,14] was used to evaluate thermal conductivity and thermal resistances.

In this paper, the thermal characteristics of soldered contacts of InGaP/Ga(In)As/Ge heterostructure with thermally conductive AlN ceramics were investigated under conditions that do not result in structural performance degradation. Soldering was carried out between Ge substrate and ceramics with preliminary preparation of their surfaces and deposition of layers of recommended metals. The thermal characteristics of the joints obtained using active solder pastes based on the binary eutectic alloy 42 mass % Sn–58 mass % Bi in the form of fluxless strip by PFARR with a thickness of 0.2 mm [15] and in the form of paste with flux KOKI TB48-M742 [16] were studied.

Before soldering, contacts were formed on the surface of the AlN-ceramics from several layers of Ti/Cu/Ni/Au metals

with a total thickness of about  $7\mu\text{m}$ , and on germanium — final gold layer ( $1\text{--}2\mu\text{m}$ ) on a sublayer of silver with a thickness of  $1.6\text{--}3.5\mu\text{m}$ . Soldering was carried out in vacuum in the temperature mode recommended by the solder manufacturer at various pressures on the elements to be soldered. The end surfaces of the samples perpendicular to the layers of the structures, which were ground and polished, were investigated.

Thermal waves in the investigated area of the sample were excited by laser radiation focused on its surface with a wavelength of  $532\text{ nm}$ , modulated in time with frequency  $5\text{ kHz}$ . The heat waves excited in the structure were detected by the deflection of the He–Ne-laser test beam traveling in the air medium above the heated surface area. The beam deflection angle varies depending on the local thermophysical properties of the irradiated sample region. To investigate the behavior of the PD signal, the sample was scanned along two coordinates in the surface plane perpendicular to the junction. The obtained PD images were used to determine the thermophysical properties and to control the homogeneity of solder contacts.

Figure 1 shows a laser PD image and a micrograph of a part of the structure surface with KOKI solder brazed at pressure of  $50\text{ g/cm}^2$  in vacuum. In the PD image, the signal from the solder layer is significantly larger than the signal from the neighboring layers (in difference to the microphotograph). In addition, significant inhomogeneities are seen within the junction layer, corresponding to regions of reduced thermal conductivity.

A three-dimensional multilayer thermal diffusion model with a Gaussian variable heat source on the surface [14] was used to determine the unknown junction parameters. The layers were assumed to be of finite thickness, but boundary conditions with thermal resistance  $R_i$  and thermal capacitive impedance  $Z_i$ , were introduced at the interfaces to model the presence of thin transition layers near the metallized surfaces formed during the soldering [17] procedure. The thermal wavelength in the Sn42Bi58 alloy for the selected modulation frequency exceeded the junction thickness, and therefore the signal near the contacts was influenced by the parameters of all components of the structure. At the same time, the thermal wavelength in germanium at  $5\text{ kHz}$  is  $47\mu\text{m}$ , and in the middle of a germanium wafer with a thickness of  $130\mu\text{m}$  the signal is determined only by the thermal conductivity of germanium and can be used to calibrate the signal at other points in the sample.

To obtain average junction parameters, cross sections of PD images perpendicular to the layer boundaries were averaged for the defect-free region with the minimum thermal barrier. Figures 2 and 3 show such cross sections for samples soldered without pressure and under pressures of  $25$  and  $50\text{ g/cm}^2$ . All curves are characterized by a significant increase in signal in the solder region, implying lower thermal conductivity than for the adjacent Ge and AlN layers. The values of the junction thermal conductivity obtained by the fitting procedure and the calculated junction thermal resistances are given in the table. The junction

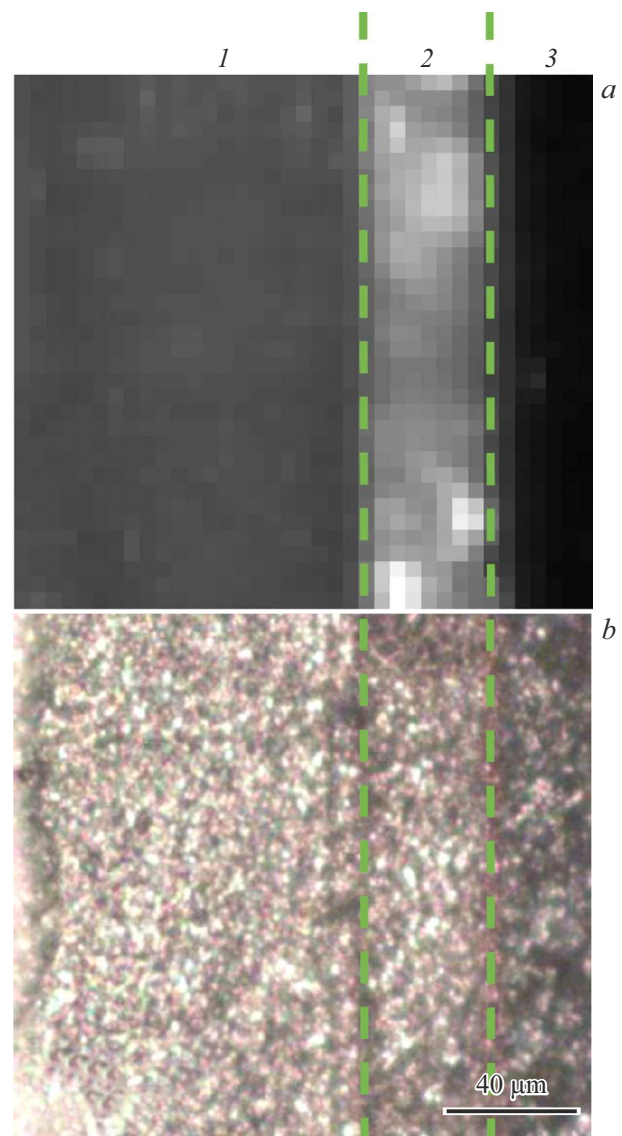


**Figure 1.** Photodeflection (*a*) and optical (*b*) images of the area around the junction using KOKI Sn42Bi58 paste. The dashed lines show the boundaries of the junction layer. 1 — germanium layer, 2 — junction, 3 — AlN-ceramic.

thermal conductivity coefficients thus determined differ from the value for bulk samples of pure Sn42Bi58 alloy of  $0.19\text{ W/(cm} \cdot \text{K)}$  [2,11]. The values are smaller for the solders obtained with KOKI flux paste, and for the solders with PFARR strip are greater than  $0.19\text{ W/(cm} \cdot \text{K)}$ . For the solders with flux, the decrease in the thermal conductivity was observed earlier [18], and the local increase in the thermal conductivity during soldering with flux free preform can be explained by the presence of two phases in the alloy: Bi and Sn, which at a given ratio of components have the form of strongly elongated (up to several tens of micrometers) regions [2]. Sn phases at small layer thicknesses can play the role of heat-conducting bridges, since the thermal conductivity of tin is  $0.65\text{ W/(cm} \cdot \text{K)}$ . It

Thermal conductivity coefficient  $K$  values obtained by the fitting procedure, and calculated thermal resistances  $R_t$  of the solder joints, taking into account the thermal impedances of the interfaces

Solder	Pressure, g/cm <sup>2</sup>					
	0		25		50	
	$K$ , W/(cm · K)	$R_t$ , cm <sup>2</sup> · K/W	$K$ , W/(cm · K)	$R_t$ , cm <sup>2</sup> · K/W	$K$ , W/(cm · K)	$R_t$ , cm <sup>2</sup> · K/W
Strip PFARR	$0.30 \pm 0.01$	$0.024 \pm 0.003$	$0.25 \pm 0.01$	$0.028 \pm 0.004$	$0.22 \pm 0.01$	$0.025 \pm 0.005$
Paste KOKI	$0.15 \pm 0.01$	$0.044 \pm 0.007$	$0.14 \pm 0.01$	$0.026 \pm 0.007$	$0.16 \pm 0.01$	$0.034 \pm 0.006$

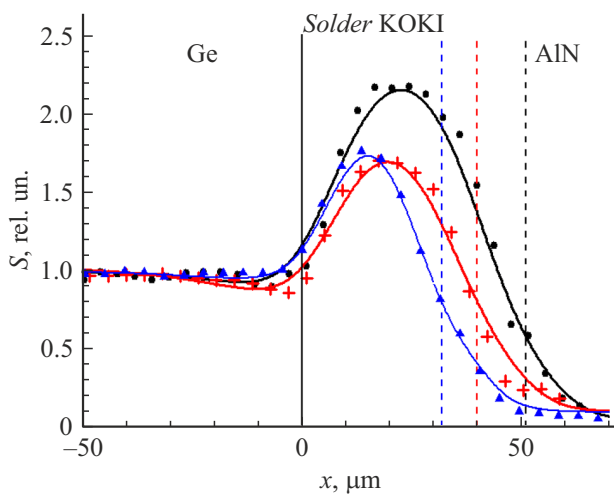


**Figure 2.** Averaged cross-sectional photodeflection image of samples soldered with Sn42Bi58 flux paste (KOKI). The symbols indicate the experimental data: circles are for the sample soldered without pressure, triangles are for the sample soldered at a pressure of 25 g/cm<sup>2</sup>, the crosses are for the sample soldered at a pressure of 50 g/cm<sup>2</sup>. The curves are the result of fitting. The vertical solid line shows - the junction boundary on the germanium side, the dashed lines show the junction boundary on the ceramic side.

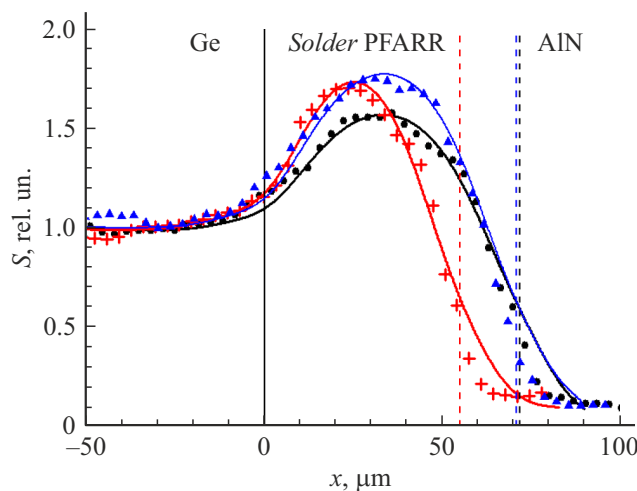


**Figure 3.** Averaged cross-sectional photodeflection image of a sample soldered with fluxless preform of Sn42Bi58 (PFARR). Designations are the same as in the Fig. 2

should be noted that this may not be true for other alloys. For example, our preliminary experiments with a fluxless strip of Sn48In52 alloy showed a decrease in the junction thermal conductivity coefficient. At the same time, this alloy has a more complex structure consisting of four phases.

For soldering with flux KOKI paste, pressure leads to a reduction in the thermal barrier. For soldering with fluxless PFARR strip, although pressure resulted in a decrease in the thickness of the solder joint, the overall thermal resistance increased insignificantly.

The results of these studies show that when selecting the material and process conditions of soldering to ensure the best heat dissipation, one should take into account the actual thermal performance of the junction layers, which may greatly differ from the performance of the basic multi-component alloys. The maximum thermal conductivity of the Sn42Bi58 flux solder junction was almost two times lower than the thermal conductivity of the junction from a fluxless strip of a similar alloy.

## Funding

The research was supported by a grant from the Russian Science Foundation №24-19-00716 (<https://rscf.ru/project/24-19-00716/>).

## Conflict of interest

The authors declare that they have no conflict of interest.

## References

- [1] M. Aamir, R. Muhammad, M. Tolouei-Rad, K. Giasin, V.V. Silberschmidt, *Solder. Surf. Mount Technol.*, **32** (2), 115 (2020). DOI: 10.1108/SSMT-11-2018-0046
- [2] I. Manasijević, L. Balanovic, U. Stamenković, M. Gorgievski, V. Čosović, *Mater. Testing*, **62** (2), 184 (2020). DOI: 10.3139/120.111470
- [3] S.R. Mang, H. Choi, H.J. Lee, *J. Korean Phys. Soc.*, **82** (11), 1105 (2023). DOI: 10.1007/s40042-023-00788-9
- [4] X. Rao, H. Liu, S. Wang, J. Song, C. Jin, C. Xiao, *Therm. Sci.*, **27** (5), 4193 (2023). DOI: 10.2298/TSCI220805061R
- [5] G. Krishnan, A. Jain, *Int. Commun. Heat Mass Transfer*, **140**, 106482 (2023). DOI: 10.1016/j.icheatmasstransfer.2022.106482

- [6] F. Jia, L. Niu, Y. Xi, Y. Qiu, H. Ma, C. Yang, *Int. J. Heat Mass Transfer*, **202**, 123719 (2023).  
DOI: 10.1016/j.jheatmass-transfer.2022.123719
- [7] N. Jiang, L. Zhang, L.L. Gao, X.-G. Song, P. He, J. Mater. Sci.: Mater. Electron., **32** (18), 22731 (2021).  
DOI: 10.1007/s10854-021-06820-7
- [8] F.Q. Hu, Q.K. Zhang, J.J. Jiang, Z.L. Song, *Mater. Lett.*, **214**, 142 (2018). DOI: 10.1016/j.matlet.2017.11.127
- [9] Q. Wang, X. Cheng, X. Wang, T. Yang, Q. Cheng, Z. Liu, Z. Lv, *Materials*, **16** (15), 5325 (2023).  
DOI: 10.3390/ma16155325
- [10] M.M. Billah, Q. Chen, *Composites B*, **129**, 162 (2017).  
DOI: 10.1016/j.compositesb.2017.07.071
- [11] K.N. Božinović, D.M. Manasijević, L.T. Balanović, M.D. Gorgievski, U.S. Stamenković, M.S. Marković, Z.D. Mladenović, *Hem. Ind.*, **75** (4), 227 (2021).  
DOI: 10.2298/HEMIND210119021B
- [12] E.S. Makarova, A.V. Asach, I.L. Tkhorzhevskiy, V.E. Fomin, A.V. Novotel'nova, V.V. Mitropov, *Semiconductors*, **56** (2), 141 (2022). DOI: 10.21883/SC.2022.02.53700.30a.
- [13] A. Glazov, K. Muratkov, *Sensors*, **23** (7), 3590 (2023).  
DOI: 10.3390/s23073590
- [14] A.L. Glazov, V.S. Kalinovskii, K.L. Muratkov, *Int. J. Heat Mass Transfer*, **120**, 870 (2018).  
DOI: 10.1016/j.jheatmasstransfer.2017.12.049
- [15] <https://pfarr.de/de/legierungsliste/>
- [16] [http://www.koki.org/pdf/B1-07\\_TB48-M742\\_E.pdf](http://www.koki.org/pdf/B1-07_TB48-M742_E.pdf)
- [17] A.L. Glazov, O.S. Vasyutinskii, *Tech. Phys. Lett.*, **40** (12), 1130 (2014). DOI: 10.1134/S1063785014120244.
- [18] A.L. Glazov, V.S. Kalinovskii, A.V. Nashchekin, K.L. Muratkov, *J. Alloys Compd.*, **800**, 23 (2019).  
DOI: 10.1016/j.jallcom.2019.06.054

*Translated by J.Savelyeva*